

Chapter 2

Mossbauer spectroscopy

2.1	Introduction	33
2.2	Principle of Mossbauer effect	34
2.3	Mossbauer Parameters	37
2.3.1	Natural Line width	38
2.3.2	Spectrometer Line width	39
2.3.3	Parabolic Effect	39
2.3.4	The Debye-Waller Factor	39
2.3.5	Isomer Shift	40
2.3.6	Magnetic Hyperfine Splitting	43
2.3.7	Electric Quadrupole Splitting	45
2.3.8	Second Order Doppler Shift	47
2.4	Mossbauer spectrometer	48
2.4.1(a)	Source	50
2.4.1(b)	Absorber	50
2.4.2	Drive Unit	51
2.4.3	Gamma Ray Detector and data acquisition System	52
2.4.4	Data Analysis	53
2.4.5	Velocity Calibration	54
2.5	Development of Mossbauer temperature Furnace	55
2.5.1	Construction of the Furnace	55
	References	59

2.1 Introduction

The interaction between a magnetic dipole or electric quadrupole moment of nucleus and a surrounding electromagnetic field lifts the degeneracy of the M states of nuclear level with spin I . The accompanying energy difference ΔE that characterizes the strength of surrounding field which induces splitting can be measured by various techniques. The techniques like ESR [1] and NMR[2] directly give the value of ΔE and PAC [3,4] operates in the time domain instead of energy domain and measures the precession frequency (ω). The measurement of nuclear spin precession frequency ω gives the information of energy difference as $\omega = \Delta E / \hbar$. This technique makes use of coupling between γ ray emission probability and spin orientation. Mossbauer spectroscopy is the technique which makes use of nuclear resonance [5, 6]. This chapter deals with the theory of hyperfine interactions and Mossbauer spectroscopic technique.

The Mossbauer Effect is based on the phenomena of recoilless emission and resonance absorption of γ rays [5]. It can provide local information about environment of particular atoms in solids, crystalline or amorphous materials. The concentration of the Mossbauer active atoms required to obtain useful spectrum is very low ($\approx 10^{14}$ to 10^{16} atoms cm^{-3}) as discussed by Williamson et al.[7], hence very dilute systems are possible to study. This technique has an excellent energy resolution amongst all. Its energy resolution is $\sim 10^{-8}$ eV in

10⁴eV. It has numerous applications in solid state physics, Nuclear Physics, Relativity, Geology, Chemistry, Biology, Medicine, Archeology etc.

2.2 Principle of Mossbauer Effect

An excited nucleus comes to its ground state by emission of γ ray, the emitted γ ray can be sensed or absorbed by another identical nucleus in the ground state and the process is called as resonance. Similar process is well known in optical resonance, the difference is only in the order of energy. In optical process the energy of electromagnetic radiation is of the order of KeV, where as γ coming from nucleus has energy thousand times greater. During emission-absorption process there is a recoil energy involved in order to conserve linear momentum. The γ emission process will provide more recoil than in the case of optical radiation. The energy of the emitted γ radiation will differ from transition energy by an amount equal to E_r . Hence the resonance probability for γ ray is less than the optical radiation. For resonance absorption the incoming photon must provide energy equal to the transition energy. R. L. Mossbauer in 1958 [8] successfully demonstrated the feasibility of observing the γ resonance fluorescence.

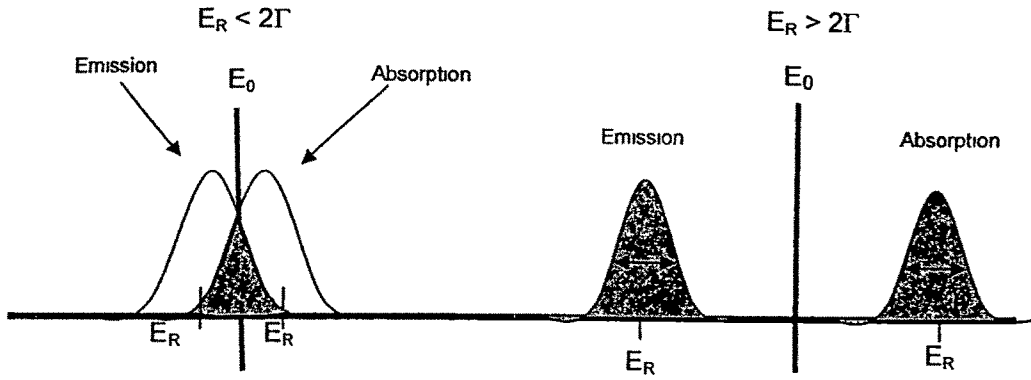


Fig 2.1 shows emission and absorption process of γ rays.

The kinetic energy associated with recoil is

$$E_r = \frac{E_0^2}{2mc^2} \quad \text{--- (1)}$$

Where E_0 is the energy of the nuclear transition, m is mass of atom, c is velocity of light, E_r is the recoil energy of the atom

Thus, the energy of emitted γ ray

$$E_\gamma = E_0 - E_r \quad \text{--- (2)}$$

Similarly in absorption process the photon should have energy

$$E_\gamma' = E_0 + E_r \quad \text{(3)}$$

Due to Doppler broadening the width of the emission and absorption lines becomes

$$\Delta = 2 (E_r K_B T)^{1/2} \quad \text{(4)}$$

where K_B is the Boltzman's constant, T is the absolute temperature of source and absorber.

In the process of emission and absorption of a photon, the total recoil energy loss is $2E_r$. Resonance occurs only if the recoil energy loss $2E_r$ is less than natural line width. Mossbauer showed that the Recoil energy E_r can be eliminated by incorporating the γ ray emitting and absorbing nuclei into well bound solids.

If the emitting or absorbing nuclei is embedded in the lattice, the recoil momentum is transferred to the lattice which induces lattice vibration. As vibrational energy levels are quantized, the recoil energy corresponding to allowed vibrations can only be transferred to the lattice. This energy transfer can induce phonon excitation in solids. The emission or absorption of the γ ray occurs in zero phonon excitation mode has no recoil, and can show the resonance. The phonon energy is $K_B\theta_D$, where θ_D is the Debye temperature of solids. If $E_r < K_B\theta_D$ a large fraction of the γ ray will produce zero phonon transition. With increase in temperature more phonons will be excited resulting in less zero phonon process. The probability of zero phonon emission or absorption of γ radiation is known as recoil free fraction

$f = \exp(-k^2 \langle X^2 \rangle)$ where k is the magnitude of wave vector, and $\langle X^2 \rangle$ is mean square displacement of the emitting or absorbing nucleus along the direction of γ ray emission.

In Debye model of lattice vibration, recoil free fraction is given by

$$f = \exp \left[\frac{-6E_r}{K_B\theta_D} \left[\frac{1}{4} + \left(\frac{T}{\theta_D} \right)^2 \int_0^{\frac{\theta_D}{T}} \frac{x dx}{e^x - 1} \right] \right] \quad (5)$$

This equation can be written as

$$f = \exp(-2W) \text{ where } W \text{ is Debye Waller factor.}$$

At very low temperature, $T < \theta_D$ it is simplified as

$$F = \exp - \left[\frac{E_R}{K_B \theta_D} \left(\frac{3}{2} + \frac{\pi^2 T^2}{\theta_0^2} \right) \right] \quad (6)$$

$$\text{For } T \geq - \frac{\theta_D}{2}$$

$$F = \exp \left[\frac{-6E_R T}{K_B \theta_D} \right] \quad (7)$$

Above equation shows that the favorable conditions for Mossbauer resonance is

- 1) low recoil energy.
- 2) Low temperature.
- 3) High Debye Temperature θ_D

2.3 Mossbauer Parameters

In a Mossbauer experiment the source or absorber is moved with respect to the other and γ ray transmission as a function of Doppler velocity is recorded. Absorption occurs at particular relative velocity. From the spectra various parameters like Isomer Shift (Chemical Shift), Quadrupole interaction, Magnetic interaction, f-fraction, line broadening, and second order dopler shift can be calculated.

2.3.1 Natural Line width

The nuclear level with finite mean life time can have uncertainty in its energy given by the equation $\Gamma = \hbar / \tau_N$. Γ is called natural line width. The frequency spectrum of the emitted γ ray has a Lorentzian distribution centered at ω_0 and half width is Γ / \hbar . The Intensity distribution of radiation at frequency ω is written as

$$I(\omega) = \frac{I_0}{1 + [(\omega - \omega_0) \hbar / \Gamma]^2}$$

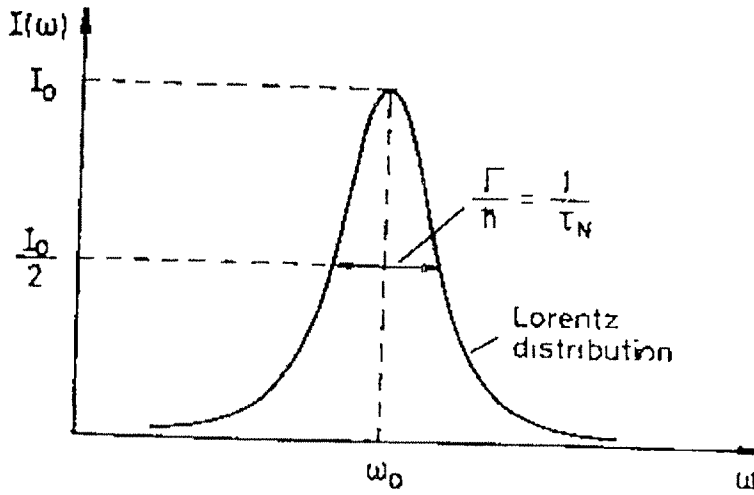


Fig : 2.2 Intensity distribution of the emitted γ ray in decay process

For ^{57}Fe nucleus, γ ray transition energy of 14.4 keV has the life time

$$\tau_N = 1.41 \times 10^{-7} \text{ s}$$

The line width $\Gamma = \hbar / \tau_N = 4.7 \times 10^{-9} \text{ eV}$

2.3.2 Spectrometer line width

In a Mossbauer experiment, the source as well as absorber has a line width Γ associated with them, and hence the minimum width observed should be 2Γ . The line widths observed in experiments are usually more than 2Γ , this is due to inhomogeneous broadening, the thickness broadening and the parabolic effect. The inhomogeneous broadening occurs due to imperfections in source and absorber. For thick absorbers the centre of the resonance saturates before the wings, thus peaks in the observed spectra gets widened [9,10].

2.3.3 Parabolic Effect

The periodic motion of source in a Mossbauer experiment causes the change in Source Detector Solid angle, hence count rate will be the parabolic function of source velocity. The magnitude of this geometric effect can be decreased by increasing source detector distance. In constant acceleration spectrometer with triangular wave, the magnitude of the parabolic effect has opposite signs in the two halves and this effect can be minimized by folding the mirror image spectra.

2.3.4 The Debye-Waller Factor

The γ ray emitting or absorbing nuclei are embedded in solids for Mossbauer experiments, and hence they are relatively strongly bound. The typical energy required to displace the atom from its lattice position is about 20eV. If the recoil energy following the emission of γ ray is not sufficient to displace, the atom

remains as it is, the γ leaves the atom in a vibration mode. When the vibrational motion of the atom is not followed by the emission, recoil energy is absorbed by the solid. The recoil energy is negligible as the mass of the crystal is $\approx 10^{20}$ times larger than that of atom. Ideal case gives unbroadened, unshifted emission line.

The ratio of the unshifted γ emission line to the total emitted γ ray line is known as Debye-Waller factor 'f'. It is temperature dependent and is largest at $T = 0K$. However, even at absolute zero, f is less than one because of zero point energy. The quantum mechanical explanation was given by Wegner et.al. [11]

2.3.5 Isomer Shift

The overlapping of the electronic wave function with the nucleus via a Coulomb interaction can affect the energy level of the states [12]. In different materials a given type of probe encounters the different electronic and chemical surroundings. The cause of the nuclear energy shift is electric monopole interaction between electrons and nucleus which is known as Isomer Shift. The isomer shift is proportional to the difference in total electron density at nucleus in source $\rho_s(0)$ and absorber $\rho_a(0)$

$$\delta = \alpha_0 [\rho_s(0) - \rho_a(0)] \quad (1)$$

Proportionality constant α_0 can be positive or negative depending nuclear parameters that can not be accurately predicted. The sensitivity in evaluating

the value of isomer shift for a given isotope is governed by α_0 and the experimental line width Γ . Theory of Isomer shift is as explained below.

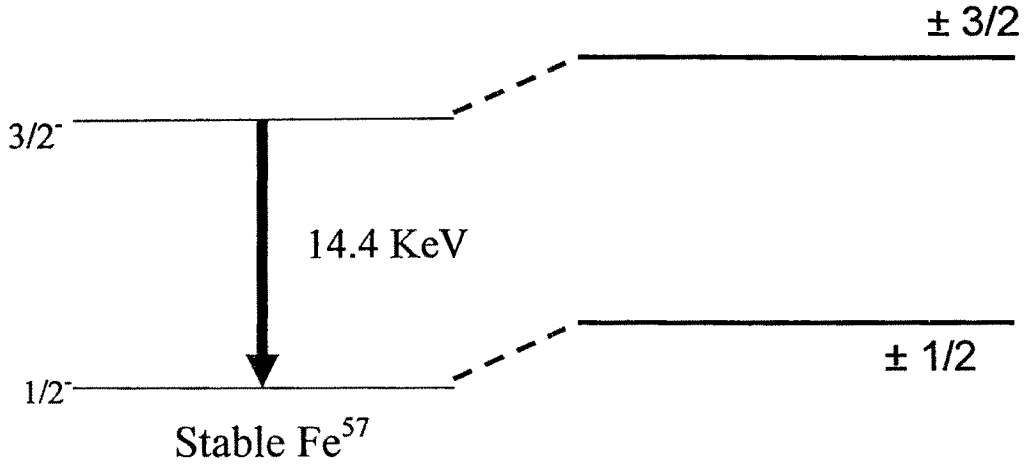


Figure : 2.3 shows level shift in Fe^{57} nucleus

The Schrodinger equation for an atomic nucleus in a Coulomb field gives ground state energy of nuclear states. The s electron wave function is symmetric round the nuclei and has finite probability at nuclei. If the nucleus is an extended object of radius R, the energy level shift in the ground state due to interaction is given by (δE_s) . The energy shift for unperturbed ground state electron wave function ψ_e is obtained by first order perturbation Hamiltonian[12]

$$\delta E_e = \langle \psi_e | H' | \psi_e \rangle \equiv \int \psi_e^*(r) H'(r) \psi_e(r) d^3r \quad (2)$$

The perturbation Hamiltonian is the difference between the point - like Coulomb potential due to the nucleus with the electron cloud. The energy of interaction between extended Coulomb potential of nucleus and electron cloud can be calculated with the help of eq(2). The potential due to nucleus can be considered as uniform charge sphere .

$$H' = e (V - V_0) \quad \text{----} \quad (3)$$

$$V_0 = \frac{1}{4\pi\epsilon_0} \frac{Ze}{r} \quad \text{----} \quad (4)$$

$$V(r < R) = \frac{Ze}{4\pi\epsilon_0} \frac{1}{R} \left(\frac{3}{2} - \frac{1}{2} \left(\frac{r}{R} \right)^2 \right) \quad \text{-----} \quad (5)$$

The distribution of the wave function for an electron within the nucleus is taken to be constant, and hence it is replaced by the probability density $|\psi_e(0)|^2$ in eq (2).

$$\delta E_e = \frac{1}{10\epsilon_0} Ze^2 R_n^2 |\psi_e(0)|^2 \quad \text{-----} \quad (6)$$

The subscript n stands for the state of nuclei. Thus we see that the value of isomer shift for a given state is the product of square of the size of the nuclei and charge density at R_n distance from nucleus. For a given material, the energy difference ΔE between excited state and ground state would be

$$\Delta E = \frac{1}{10\epsilon_0} Ze^2 |\psi_e(0)|^2 (R_1^2 - R_0^2) \quad \text{-----} \quad (7)$$

This equation is similar to eq (1). Isomer Shift can be positive or negative depending on whether the excited state has a larger or smaller radius than the ground state. For more practical purpose the eq (6) is modified

$$\Delta E = \frac{1}{10\epsilon_0} Z_e^2 [|\psi_A(0)|^2 - |\psi_S(0)|^2] [\langle r_e^2 \rangle - \langle r_s^2 \rangle] \quad \text{---} \quad (8)$$

For a nonzero isomer shift to occur the following condition must be satisfied.

$$|\psi_A(0)|^2 - |\psi_S(0)|^2 \neq 0 \quad \text{---} \quad (9)$$

$$\langle r_e^2 \rangle - \langle r_s^2 \rangle \neq 0 \quad \text{----} \quad (10)$$

For Fe^{57} nucleus, $\langle r_e^2 \rangle - \langle r_s^2 \rangle$ is negative, hence nucleus has a smaller radius in the excited state than the ground state.

2.3.6 Magnetic Hyperfine splitting.

The presence of a magnetic field H at the nucleus of the Mossbauer active isotope will produce a splitting of nuclear levels through magnetic Dipole interaction, this is called nuclear Zeeman effect. The nucleus with spin I and magnetic moment μ in the presence of magnetic field H experiences a torque due to which the moment tries to align with the field. The interaction energy associated with it is given by Hamiltonian [13]

$$H_M = -g\mu_N \cdot H \cdot I_z \quad \text{----} (1)$$

Where g is the nuclear lande factor, μ_N is nuclear magnetic moment and I_z is the z component of I in the direction of H .

The Magnetic Hyperfine field H exists at the nucleus can be written as

$$H = H_0 - DM + \frac{4}{3\pi} M + H_S + H_L + H_D \quad \text{-----}(2)$$

Where H_0 is the externally applied field, H_S is the interaction between electron spin density and the nucleus (Fermi contact term), H_L is contribution arising from orbital magnetic moment and H_D is dipole interaction of the nucleus with spin moment. Fig shows schematic diagram of magnetic Hyperfine splitting of Fe^{57} .

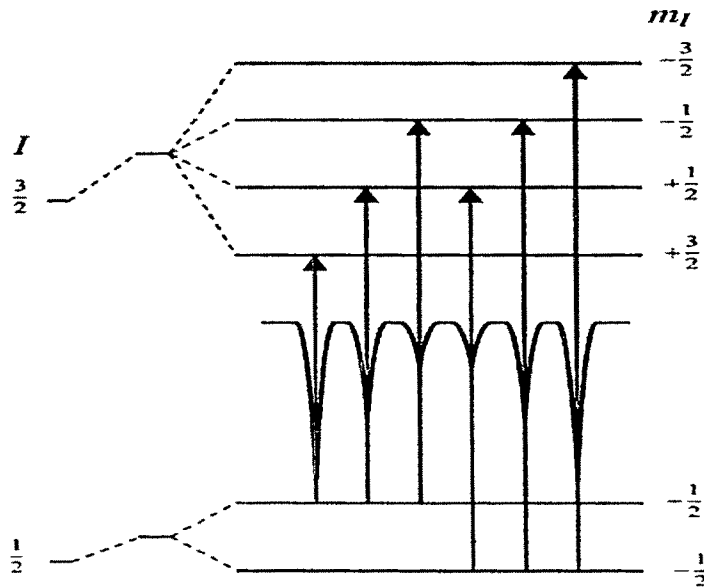


Figure 2.4 Magnetic Hyperfine splitting of Fe^{57}

Only six transitions are allowed by M1 selection rules, it follows that the radiation are pure M1. The transition energy associated are

$$h\omega (M_e \rightarrow M_g) = h\omega_0 - \left(\frac{\mu_e}{I_e} M_e - \frac{\mu_g}{I_g} M_g \right) H \quad \text{-----}(3)$$

Each of the transitions that correspond to interaction energy is scanned by moving source. The resonance velocity for moving source are written as

$$\hbar\omega\left(1+\frac{v_{res}}{c}\right)=\hbar\omega_0-\left(\frac{\mu_e}{I_e}M_e-\frac{\mu_g}{I_g}M_g\right)H \quad \text{----(4)}$$

2.3.7 Electric Quadrupole Splitting

Electric Quadrupole interaction in the system arises due to the interaction between the quadrupole moment of nucleus and the electric field gradient produced by the asymmetric electronic charge distribution around it. The Electric quadrupole interaction in Mossbauer active nucleus was well explained by Gonser et. al.[13] and Dunlop et. al. [14] The Quadrupole moment (Q) of the nucleus strictly depends on I. Nuclei having 0 or ½ spins are spherically symmetric and don't assume any quadrupole moment.

Electric field gradient is a product of gradient operator and a directional component of electric field, and is a tensor quantity. Diagonal components of electric field gradient are written as $\partial^2V/\partial x^2 = V_{xx}$, $\partial^2V/\partial y^2 = V_{yy}$, $\partial^2V/\partial z^2 = V_{zz}$.These components obey the Laplace's equation $V_{xx} + V_{yy} + V_{zz} = 0$. An arbitrarily chosen component V_{xx} remains independent of other two.

The asymmetry parameter η for a given component is

$$\eta = \frac{V_{xx}-V_{yy}}{V_{zz}} \quad \text{----(1)}$$

The asymmetry parameter is used in calculating Electric Field Gradient (EFG) set up by Crystal surrounding.

The quadrupole moment of the nucleus interacts with the electric field gradient. This interaction lifts the degeneracy of the excited as well as the ground states and splits it into $2I+1$ sub levels. The eigen values of the states are obtained by the interaction Hamiltonian

$$E_Q = \frac{eqQV_z}{4I(2I-1)} [3m_I^2 - I(I+1)] \left[1 + \frac{\eta^2}{3} \right]^{1/2} \quad \text{--- (2)}$$

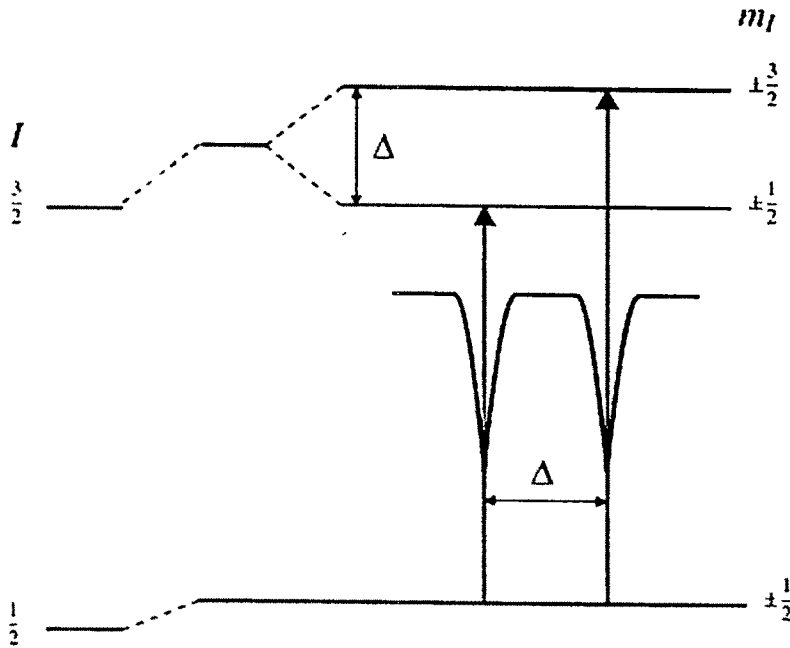


Figure 2.5 shows the splitting of excited state in ^{57}Fe ($I = 3/2$)

The spectrum will consist of two components corresponding to $\pm 3/2 \rightarrow \pm 1/2$ and $\pm 1/2 \rightarrow \pm 1/2$ transition having the eigen value

$$E_Q = \frac{eqQV}{4} \left[1 + \frac{\eta^2}{3} \right]^{1/2} \quad \text{----- (3)}$$

In practice, Quadrupole doublet can be resolved if the following condition satisfied

$$|E_Q(\pm 3/2 \rightarrow \pm 1/2)| + |E_Q(\pm 1/2 \rightarrow \pm 1/2)| >> 2\Gamma \quad \text{----- (4)}$$

where Γ is a natural line width.

2.3.8 Second Order Doppler Shift

Pound and Rebka [15] and Josephson [16] discussed the temperature dependence in the isomer shift. The relativistic equation for Doppler Effect on an emitting photon gives the observed frequency.

$$\nu' = \nu \left(1 - \frac{v}{C} \right) \left(1 - \frac{v^2}{C^2} \right)^{-1/2} \quad \text{----- (1)}$$

This equation is approximated as

$$\nu' = \nu \left(1 - \frac{V}{C} \right) \left(1 + \frac{V^2}{2C^2} \right) \quad \text{----- (2)}$$

Where ν is the frequency of stationary system.

The atom vibrating along the direction of γ ray emission will have a zero velocity over the life time of the state. So first order term don't contribute. The contribution of the second order term is given by

$$v' = v \left(1 + \frac{\langle V^2 \rangle}{2C^2} \right) \quad \text{----- (3)}$$

This can give rise to shift in to Mossbauer lines given by

$$\frac{\delta E_R}{E_R} = - \frac{\langle V^2 \rangle}{2C^2} \quad \text{----- (4)}$$

This is referred as a second order Doppler shift.

The isomer shift can be written as $\sigma = \sigma_c + \sigma_{\text{SOD}}$, where σ_c is shift due to chemical environment and σ_{SOD} is that due to second order Doppler shift.

The contribution of SOD can be estimated if Debye temperature of source and absorber are known.

2.4 Mossbauer spectrometer

There are two different methods of measuring the transmitted γ ray intensities.

- a) At constant velocity measuring the total number of transmitted photons for a fixed time.
- b) At constant acceleration the whole velocity range is scanned.

Mossbauer spectrometer are usually operates in transmission geometry using a constant acceleration drive. In this geometry the source is vibrated whose velocity (V) linearly increases or decreases to Doppler modulate the gamma

energy. The corresponding data of absorption in successive half periods of oscillation are stored with the help of multichannel analyzer in a Multi Scaling Mode (MCS). The switching of registered channel for data acquisition is synchronized with linearly changing speed of the source by a synchronization pulse.

Mossbauer spectrometer consists of following major parts as shown in fig.

1. Mossbauer source and Absorber.
2. Drive unit.
3. Gamma ray detector.
4. Data acquisition system.

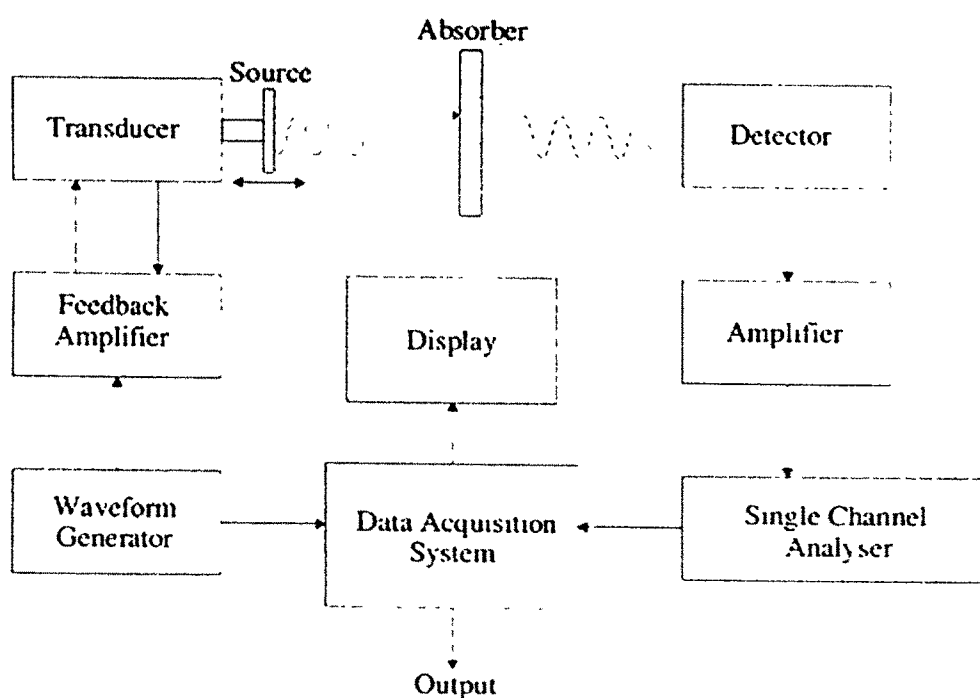


Figure 2.6 shows block diagram of Mossbauer spectrometer

2.4.1 Mossbauer Source and Absorber

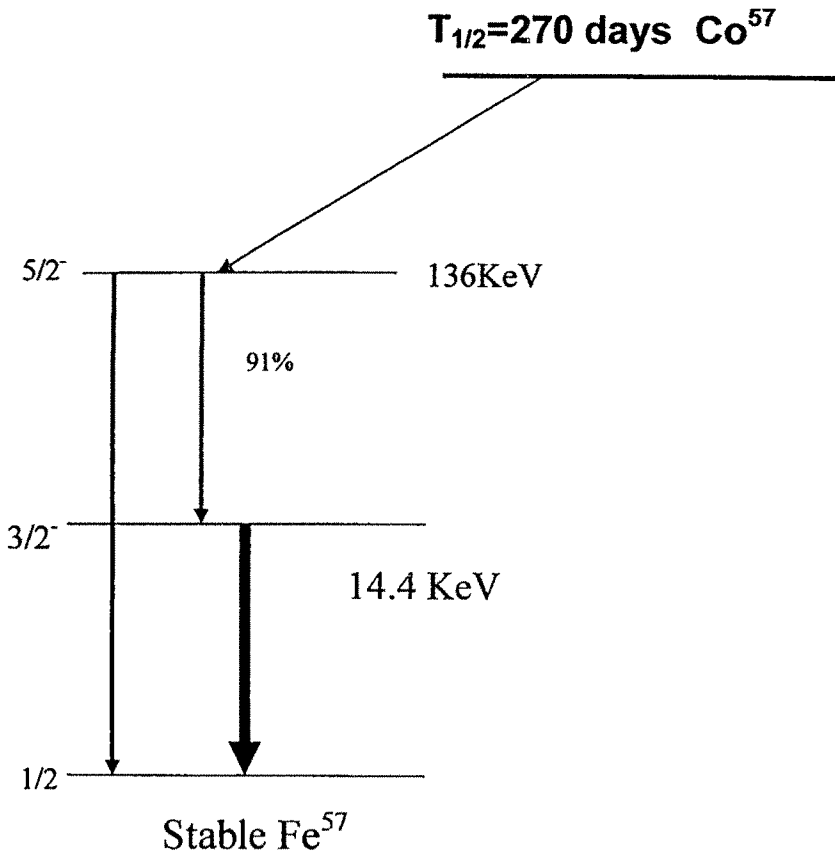
a) Source

The source used was ^{57}Co in a rhodium matrix. Rhodium is a cubic and non magnetic metal which provides solid environment to ^{57}Co with high recoil free fraction. ^{57}Co has a half life 271.7 days and decays via electron capture to $I = 5/2$ state of the ^{57}Fe . This daughter nucleus is in excited state and comes to its ground state by emitting three different γ rays of 14.4 KeV, 123 KeV and 137 KeV. The 14.4 KeV γ transition corresponds to $3/2 \rightarrow 1/2$ levels.

The mean life time of this $I = 3/2$ state is 97.8ns which corresponds to a natural line width of 0.194 mm/sec. For accurate measurement of the Mossbauer parameters, source should have line width corresponds to natural line width. ^{57}Co in a Rh matrix is one of the Mossbauer source which has a high recoil free fraction and narrow line width. Decay scheme of the ^{57}Co is as shown in the figure below.

b) Absorber

Mossbauer absorbers used in the present study were dilute alloys of Germanium semiconductor. Natural abundance of ^{57}Fe in iron metal is 2% (i.e. 2×10^{13} Fe^{57} nuclei/gm mol). In order to get a good signal to noise ratio a minimum concentration of Mossbauer active atom is needed. The absorber samples in our study were made from 95% enriched iron 57 isotopes. The samples for Mossbauer study were taken in the powder form and spread uniformly in a 1.2 cm^2 area to make the absorbers.

Figure 2.7 Decay scheme of Co^{57}

2.4.2 Drive Unit

Drive unit consists of a function generator, Drive amplifier and a transducer. The source is mounted on a transducer which oscillates according to drive current from amplifier. The transducer is made up of moving coil in a constant magnetic field. Motion of the transducer excels induces current in sensing coil that is compared to reference current ramp. The difference (error) signal is feedback to drive current amplifier and consequently correction is done.

The reference current is triangular function of time with a linear rise from $-I_0$ to $+I_0$ with fly back to $-I_0$. The corresponding velocity is therefore triangular function of time from $-V_0$ to V_0 . The maximum velocity imparted to the source is $\pm 25 \text{ mm/sec}$. The ramp generator circuit is triggered by synchronous signal from MCS.

2.4.3 Gamma ray detector and data acquisition system

The detector used is a sealed proportional counter, filled with mixture of 90% Krypton and 10% methane gas. The applied bias voltage was around 2KV. Detector attached with pre-amplifier and a low-noise active filter amplifier, gives pulses of different voltage according to incident γ ray energy. The amplifier out put was fed to the Multi Channel Analyzer (MCA). Energy selection for 14.4 KeV γ ray was done by a Single Channel Analyzer (SCA), lower level discriminator (LLD) and upper level discriminator (ULD) is set through software gating in a pulse height analysis (PHA) mode of MCA.

Gated pulses are converted into logic pulse in an Analog to Digital converter (ADC). The signal in the form of transmitted counts are accumulated in 1024 channels of MCA in a multi scaling mode synchronized with transducer acceleration. For one complete cycle of transducer oscillation two spectra can be recorded, one is for positive acceleration and other is for negative acceleration. As it operates in constant acceleration mode, time interval is constant for all

velocity intervals hence each channel records the data for an equal time duration. Synchronization of transducer and Multi Channel Analyzer is done by clock pulse generated by MCA. During the analysis full spectrum is folded around the centre point to produce single spectrum. Folding doubles the counts and flattens the background profile produced by the difference in intensity of source radiation.

2.4.4 Data Analysis

The data acquired in MCA has a combined effect of Quadrupole and Magnetic interaction, it is plotted as no of counts versus channel no. This data was analyzed with lorentzian curve fitting program developed by Meerwal [17]. The minimum in χ^2 is tested by specifying in a random parameters.

The lorentzian curve fitting program uses the mathematical equation

$$F(x, P) = P_{L+1} + \sum_{j=3m-2}^j P(P_j, P_{j+1}, P_{j+2}, x)$$

Where P_{L+1} represents a background and P_j, P_{j+1}, P_{j+2} are centroid, peak height and FWHM of the m^{th} line. The function F has the lorentzian form.

$$F(P_j, P_{j+1}, P_{j+2}, x) = P_{j+1} \left\{ \frac{4(x - P_j)^2}{P_{j+2}} + 1 \right\}$$

The computer analysis of the Mossbauer data gives peak position, intensity and Line width. From These parameters the value of the Isomer shifts, Quadrupole

Splitting and Magnetic interaction strength. Site population can also be calculated.

2.4.5 Velocity Calibration

The velocity calibration was done using natural Iron as an absorber and Co^{57} as source. It was calculated as 0.028 mm/sec per channel. The resolution of our spectrometer was 0.28 mm/sec. Fig 2.8 shows the calibration spectra of the same.

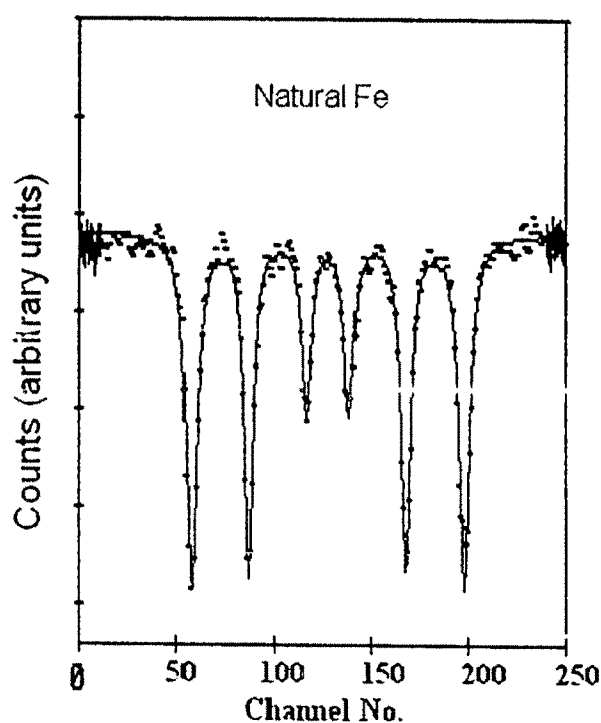


Fig 2.8 shows the calibration spectra of Natural Iron

2.5 Development of Mossbauer temperature Furnace

Mossbauer study at elevated temperature helps in evaluating various parameters like transition temperature T_c of the magnetic phase, trend of the Isomer shift and hence contribution of Second Order Doppler Shift, Phase dissociation temperature etc. For that the high temperature vacuum furnace with temperature stability and accuracy is very essential. Fig shows the block diagram of the furnace designed and developed in house.

2.5.1 Construction of the furnace

The high temperature vacuum furnace was constructed to record Mossbauer spectra of the sample up to 800°K. Fig 2.1.7 shows the block diagram of the furnace.

As shown in the figure, A indicates the vacuum outlet arrangement. Upto 10^{-5} torr pressure could be achieved in the furnace through the vacuum system attached to it. The purpose of high vacuum in a furnace was just to prevent the sample from oxidation at high temperatures. The outer jacket of the furnace (B) was made of Aluminum in a hollow cylindrical form. The thickness was kept about 1.5 cm and its outer diameter (OD) was kept around 10 cm. Inside this jacket the cylindrical ceramic heat shield of OD 6.5 cm was taken. The gap between heat shield and outer jacket was filled with glass wool to provide substantial thermal inertia.

The Nichrome heater coil of 22 gauge was used for heating the sample. Heater operating voltage and current was 230V / 5 Amp respectively. It was wound on a mica sheet, which was wrapped on the aluminum hollow cylinder (F) of OD 2.5 cm. At the center of this cylinder the sample holder (D) arrangement was made. A Mylar window was used on both side of the outer aluminum jacket, so that the gamma rays can transmit.

The Cr/Al Thermocouple was used to measure the temperature near the sample holder. The thermocouple was calibrated initially before use. This thermocouple was attached to the digital temperature controller whose accuracy is $\pm 1^{\circ}\text{C}$.

The whole furnace assembly was then covered with copper spiral pipe through which water can be flowed to prevent heating.

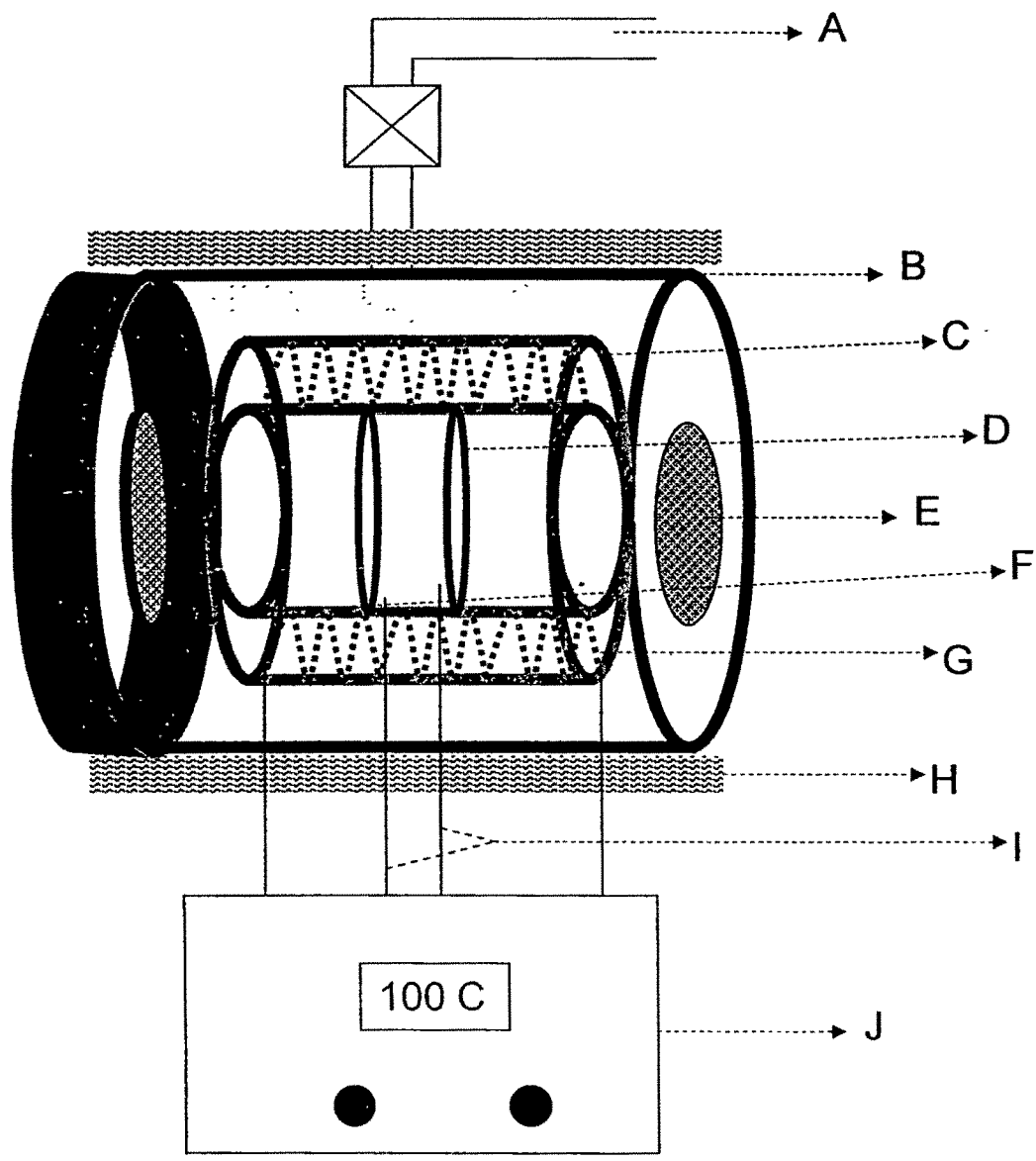


Fig. 2.9 High temperature Furnace for Mossbauer Spectroscopy

Where,

A : Vacuum Out let.

B : Cylindrical outer jacket made up of aluminum

C : Ceramic heat shield.

D : Aluminum sample holder.

E : Mylar window of 0.5 mm thickness.

F : Cylindrical Aluminum jacket.

G : Nichrome Wire (Heater).

H : Cooper cooling pipe wounded round the furnace.

I : Cr/ Al temperature sensor.

J : Temperature controller.

References

1. K. A. McLauchlan, *Magnetic Resonance* (Clerendon Press, Oxford)(1972).
2. H. Ackermann, D.Dubbers and H.J.Stockmann, *Adv. Nucl.Quadrupole Resonance*, Vol III, ed. J.A.S.Smith (Heyden London) pp. 1-66 (1978).
3. H. Frauenfelder and R.M.Steffen, in: *Alpha,Beta,Gamma ray spectroscopy*, Vol. 2, ed. K. Sieghban (North Holland, Amsterdam) p. 997. (1965).
4. W. D. Hamilton, *The Electromagnetic Interaction in Nuclear Spectrscopy* (North Holland, Amsterdam)1975.
5. G. K. Werthiem, "Mossbauer Effect" Academic Press, London,1964.
6. N .N. Greenwood, and T. C. Gibbs, " Mossbauer Spectroscopy" ,Chapmann and Hall Ltd., London, (1971) 19.
7. D. L. Williamson, L. Niesen, G. Weyer, R.Sielemann,G.Langouche, *Hyperfine Interaction of defects in semiconductors*, ed. by Elsevier publisher, Netherlands (1992).
8. R.L.Mossbauer., *Z.Phys.* Vol. 151, (1958) p.124.
9. K.Alder., *Phys. Rev.* 84 (1951), p-369.
10. L. H .Schwartz., "Application of Mossbauer Spectroscopy"., ed. by R.L.Cohen, Academic Press, vol. I, p-37.
11. H.Wegner , *Der Mossbauer Effekt und seine Anwendungen in Physik und Chemie*, ed. By Hochshultaschenbuch. Bibliographisches Institut, Mannheim.

12. G. K. Shenoy and F.E.Wagner, eds, 1978, Mossbauer Isomer shifts
(North - Holland, Amsterdam).
13. U. Gonser., 1975, in Mossbauer Spectroscopy, ed. U. Gonser
(Springer, New Yourk), p.1
14. B.D.Dunlap, Mossbauer Effect Data Index 1970 eds J.G.Stevens and
V.E.Stevens (1972) p25.
15. R. V. Pound and G. A. Rebka, Phys.Rev.Lett, 4 (1960), p-274.
16. B. D. Josephsen, Phys.Rev.Lett,4(1960), p-341.
17. E.V.Meerwal, Com.Phys. Commun., 9(1975) 117.